

ON RELIABLE AND UNRELIABLE NUMERICAL METHODS FOR THE SIMULATION OF SECONDARY SETTLING TANKS IN WASTEWATER TREATMENT

RAIMUND BÜRGER^{A,*}, STEFAN DIEHL^B, SEBASTIAN FARÅS^B, AND INGMAR NOPENS^C

ABSTRACT. A one-dimensional model for the sedimentation-compression-dispersion process in the secondary settling tank can be expressed as a nonlinear strongly degenerate parabolic partial differential equation (PDE), which has coefficients with spatial discontinuities. Reliable numerical methods for simulation produce approximate solutions that converge to the physically relevant solution of the PDE as the discretization is refined. We focus on two such methods and assess their performance via simulations for two scenarios. One method is provably convergent and is used as a reference method. The other method is less efficient in reducing numerical errors, but faster and more easily implemented. Furthermore, we demonstrate some pitfalls when deriving numerical methods for this type of PDE and can thereby rule out certain methods as unsuitable; among others, the wide-spread Takács method.

1. INTRODUCTION

The key operation in many wastewater treatment plants (WWTPs) for the purification of industrial and domestic sewage is the activated sludge process in biological reactors and secondary settling tanks (SSTs). Despite a century of usage and experience, the sedimentation process in the SST is still a challenge in modelling the full-scale operation of wastewater treatment plants (WWTPs). In modelling the activated sludge process, biological reactors have traditionally received more attention than SSTs. This emphasis has mainly been motivated by the wish to predict the effluent quality while the role of the SST model was to create a reasonable sludge balance. Most commercial simulators, however, do not provide reliable simulation models in the sense that there is no guarantee that the simulations satisfy fundamental physical properties under all conditions. From a practical point of view, current SST simulation models tend to be inaccurate under wet weather conditions where a significant amount of sludge mass is recycled within the plant.

Date: January 18, 2012.

Key words and phrases. Secondary settling tank, wastewater treatment plant, numerical method, method of lines, Godunov flux, efficiency.

*Corresponding author.

^ACI²MA and Departamento de Ingeniería Matemática, Facultad de Ciencias Físicas y Matemáticas, Universidad de Concepción, Casilla 160-C, Concepción, Chile. E-Mail: rburger@ing-mat.udec.cl.

^BCentre for Mathematical Sciences, Lund University, P.O. Box 118, S-221 00 Lund, Sweden. E-Mail: diehl@maths.lth.se, faras@maths.lth.se.

^CBIOMATH, Department of Mathematical Modelling, Statistics and Bioinformatics, Ghent University, Coupure Links 653, B-9000 Gent, Belgium. E-Mail: ingmar.nopens@ugent.be.

In the traditional layer models, the development of which experienced a breakthrough by Takács et al. (1991), the numerical method is written up directly by a mass balance reasoning between the layers and often by the addition of heuristic assumptions to fix problems or to try to adjust the simulator to data. Recent attempts to improve SST simulation models in this way are presented by Verdickt et al. (2005), Nocoń (2006), Plósz et al. (2007), Abusam & Keesman (2009), David et al. (2009a, 2009b) and Guo et al. (2010).

From a consistent modelling point of view, common simulation models frequently lack a proved connection to underlying physical principles. The conservation law of mass can be captured by a mathematical model in integral form or as a partial differential equation (PDE), which is nonlinear and may have discontinuous solutions. Another physical principle is that only stable discontinuities should appear in the solution, which means that a so-called entropy condition must be imposed. The model PDE cannot be expected to have a closed-form solution, so a numerical method is needed. It should be derived from the integral form of the model equation and produce approximate solutions that converge to the exact solution as the discretization is refined (Bürger et al., 2011). Such a numerical method is called *reliable*. To date, the only published numerical method with a proof of convergence for this type of PDE (without dispersion) was presented by Bürger et al. (2005). We denote this Method EO, since it utilizes the numerical flux by Engquist & Osher (1981). Method EO was also used earlier by De Clercq et al. (2008).

Bürger et al. (2011) proposed a one-dimensional (1D) SST model that captures most of the phenomena addressed by previous 1D models, namely hindered settling, compression at high concentrations, and dispersion around the inlet due to turbulence. In a subsequent paper, Bürger et al. (2012) derived a numerical method and described all details necessary for its implementation. This numerical method is here called Method G, since its numerical flux is based on the well-known flux by Godunov (1959). Godunov's flux was introduced for the simulation of SSTs by Diehl & Jeppsson (1998) and it is also used by Plósz et al. (2007). Method G is more easily implemented and requires fewer computations than Method EO. The speed is an important aspect when the SST simulator should be included in a simulator of an entire WWTP. Proving convergence for a numerical method for this type of PDE is difficult. Since Method EO is proved reliable (at least for constant feed inputs), we use it here as a reference method.

The first purpose of the current work is to compare Method G with Method EO and thereby strengthen our hypothesis that also Method G is reliable. The second purpose is to investigate accuracy and required CPU times for the two methods. The third purpose is to enlighten the inherent difficulties of obtaining a reliable numerical method for the PDE under consideration. Some pitfalls (like errors in the implementation of numerical methods) will be demonstrated. In particular, we will investigate the Stenstrom-Vitasovic-Takács minimum-flux used in the well-known simulation method by Takács et al. (1991), and demonstrate that this method may lead to erroneous numerical results.

The remainder of the paper is organized as follows. In Section 2, the model and the fundamentals of reliable numerical methods are reviewed. The comparison between Method G and Method EO can be found in Section 3. Pitfalls and unsuitable numerical methods are discussed in Section 4 and conclusions can be found in Section 5.

2. THE MODEL AND NUMERICAL METHODS

2.1. The model in PDE form. Suppose that the sludge concentration C is horizontally constant. Then C can be treated as a function of depth z and time t only. Let A denote the constant cross-sectional area of the SST and Q_f and C_f the volumetric flow rate and concentration of the feed inlet, respectively. Conservation of mass yields the model PDE

$$\frac{\partial C}{\partial t} + \frac{\partial}{\partial z} F(C, z, t) = \frac{\partial}{\partial z} \left((\gamma(z)d_{\text{comp}}(C) + d_{\text{disp}}(z, Q_f)) \frac{\partial C}{\partial z} \right) + \frac{Q_f(t)C_f(t)}{A} \delta(z). \quad (1)$$

Here, $\gamma(z)$ is a characteristic function which equals 1 inside the tank and zero outside. The last term is a point source, where δ is the Dirac delta distribution. Dispersion near the feed inlet is modelled by d_{disp} and compression by d_{comp} . We assume that $d_{\text{comp}}(C) \neq 0$ only for concentrations above a critical concentration C_c at which the flocs begin to form a compressible network. If f_{bk} denotes the Kynch batch flux function $f_{\text{bk}}(C) = Cv_{\text{hs}}(C)$, where v_{hs} is the hindered settling velocity, then the flux function F depends discontinuously on z in the following way:

$$F(C, z, t) = \begin{cases} -Q_e(t)C/A & \text{for } z < -H & \text{(effluent zone),} \\ f_{\text{bk}}(C) - Q_e(t)C/A & \text{for } -H \leq z < 0 & \text{(clarification zone),} \\ f_{\text{bk}}(C) + Q_u(t)C/A & \text{for } 0 < z \leq B & \text{(thickening zone),} \\ Q_u(t)C/A & \text{for } z > B & \text{(underflow zone),} \end{cases} \quad (2)$$

where H is the height of the clarification zone and B is the depth of the thickening zone. The volumetric flow rates in the effluent and the underflow are given by $Q_e \geq 0$ and $Q_u \geq 0$, respectively, and satisfy $Q_f = Q_e + Q_u$.

Our model thus consists of the PDE (1) and three constitutive relations for f_{bk} , d_{comp} and d_{disp} . It is well known that solutions $C = C(z, t)$ of (1) may contain discontinuities, which may either move, such as rising or falling jumps in concentration in the clarification and thickening zones, or be stationary, as are concentration jumps caused by changes in the definition of (2) across the boundaries of the four zones. Therefore, Equation (1) has to be interpreted in the so-called weak sense. Furthermore, to obtain a unique solution for given initial data, an additional physical principle, called the *entropy condition*, must be satisfied at every discontinuity (Bürger et al., 2005; Diehl, 2009).

2.2. The model in integral form and method-of-lines formulation. Because of possible discontinuities in the solution, the derivatives in Equation (1) are not classical ones, which means that it is not straightforward to use any finite difference approximation for the derivatives. The formulation of a reliable numerical method starts most conveniently from a more fundamental form of the conservation law than the PDE (1), namely the integral form:

$$\frac{d}{dt} \int_{z_1}^{z_2} C(z, t) dz = \Phi|_{z=z_1} - \Phi|_{z=z_2} + \frac{1}{A} \int_{z_1}^{z_2} Q_f(t)C_f(t)\delta(z) dz, \quad (3)$$

where (z_1, z_2) is an arbitrary interval of the z -axis (a layer in the method) and the flux Φ is

$$\Phi \left(C, \frac{\partial C}{\partial z}, z, t \right) = F(C, z, t) - (\gamma(z)d_{\text{comp}}(C) + d_{\text{disp}}(z, Q_f)) \frac{\partial C}{\partial z}. \quad (4)$$

Note that (3), (4) is equivalent to the PDE (1), if the latter is interpreted in the weak sense.

The z -axis is divided into a finite number of layers and a method-of-lines formulation of the numerical method is possible, i.e. a system of ordinary differential equations (ODEs). Precisely, we subdivide the SST into N internal layers, so that each layer has the depth $\Delta z = (B + H)/N$, and assume that the boundaries between the layers are $z_j := j\Delta z - H$ for $j = 0, \dots, N$. In particular, $z_0 = -H$ and $z_N = B$. We will refer to “layer j ” as the interval $[z_{j-1}, z_j]$. Define $j_f := \lceil H/\Delta z \rceil$, which is equal to the smallest integer larger or equal to $H/\Delta z$. Then the location of the feed inlet ($z = 0$) is in the interval $(z_{j_f-1}, z_{j_f}]$ and the corresponding layer is called the “feed layer”. In the formulation of the numerical scheme we add two layers to both the top and bottom corresponding to the effluent and underflow zones, respectively. Thus, our computational domain is composed of $N+4$ intervals of length Δz , enclosed by the points z_j , $j = -2, \dots, N+2$.

The method-of-lines formulation is

$$\begin{aligned} \frac{dC_j}{dt} = & -\frac{F_j^{\text{num}} - F_{j-1}^{\text{num}}}{\Delta z} + \frac{1}{\Delta z} \left(J_{\text{disp},j}^{\text{num}} - J_{\text{disp},j-1}^{\text{num}} + J_{\text{comp},j}^{\text{num}} - J_{\text{comp},j-1}^{\text{num}} \right) \\ & + \frac{Q_f C_f}{A \Delta z} \delta_{j,j_f}, \quad j = -1, \dots, N+2, \end{aligned} \quad (5)$$

where $C_j(t)$ is the average concentration in layer j at time t , and δ_{j,j_f} is the standard Kronecker symbol with $\delta_{j,j_f} = 1$ if $j = j_f$ and $\delta_{j,j_f} = 0$ otherwise. The expressions F_j^{num} , $J_{\text{disp},j}^{\text{num}}$ and $J_{\text{comp},j}^{\text{num}}$ are numerical approximations of the three respective terms of Φ in (4). We refer to Bürger et al. (2012) for the derivation and implementation of the method. In Bürger et al. (2011), we emphasized some fundamental principles (CFL condition, consistency and entropy satisfying numerical flux) for PDE solvers for (1). We will here go into more detail and discuss the monotonicity property of the numerical method, which is central for proving convergence.

2.3. Numerical fluxes. In the spatial discretization, F demands some extra care. Its numerical approximation is called the *numerical flux*, denoted by F^{num} . This quantity will in general depend on the adjacent layer concentrations C_j and C_{j+1} , i.e.,

$$F_j^{\text{num}}(C_j(t), C_{j+1}(t), t) \approx F(C(z_j, t), z_j, t).$$

There are several reasonable choices of the numerical flux F_j^{num} , and several restrictions that must be met to ensure convergence to the exact solution. These issues are broadly discussed in textbooks on numerical schemes for conservation laws (see, e.g., LeVeque, 1992, 2002; Holden & Risebro, 2007). One basic requirement is that the numerical flux should be consistent with the exact flux, i.e.,

$$F_j^{\text{num}}(C, C, t) = F(C, z_j, t) \quad \text{for all } C, j, t. \quad (6)$$

Two alternative choices are the consistent numerical fluxes due to Godunov (1959) and Engquist & Osher (1981), leading to slightly different numerical schemes. Once a formula for the numerical flux has been chosen, there are two principle ways to proceed. For simplicity of description, consider only the thickening zone ($0 < z < B$) (the clarification-zone case is analogous). The flux in the thickening zone f is given by the superposition of the nonlinear function f_{bk} and a linear term due to the downward bulk flow (cf. (2)):

$$f(C, t) = f_{\text{bk}}(C) + Q_u(t)C/A.$$

The first way is to apply the Engquist-Osher (or Godunov) formula directly on the total flux f . This was done with the Engquist-Osher formula by Bürger et al. (2005), whereas Diehl & Jeppsson (1998) used the Godunov formula. The second way is to apply the chosen formula to the two terms of the flux function f separately; partly on the nonlinear term f_{bk} , and partly on the linear term $Q_{\text{u}}C/A$. This implies that the linear term is discretized in an upwind fashion, i.e., $Q_{\text{u}}C/A$ is replaced by $Q_{\text{u}}C_j/A$. (For the clarification zone $-Q_{\text{e}}C/A$ is replaced by $-Q_{\text{e}}C_{j+1}/A$.)

To elucidate the benefits of the second alternative, observe that the computations of both the Godunov and Engquist-Osher numerical fluxes rely on the knowledge of the local extrema of the function they are applied on. Consider again the thickening zone. Since Q_{u} may vary with time, so may the local extrema (with respect to C) of $f(C, Q_{\text{u}})$. Consequently, the first alternative requires us to keep track of these extrema over time. On the other hand, f_{bk} is the same function throughout the simulation, so in the second alternative it suffices to determine the extrema just once in an initializing step. This means easier implementation, fewer computations, and thereby faster simulations. The last property comes, however, at the cost of increased numerical errors; see Section 3.

We have so far discussed four possible ways of computing F_j^{num} . In light of the convergence results by Bürger et al. (2005), we choose as the numerical flux in Method EO the Engquist-Osher formula on the total flux f (for the thickening zone):

$$F_j^{\text{num,EO}} = F^{\text{num,EO}}(C_j, C_{j+1}, t) := \frac{1}{2} \left(f(C_j, t) + f(C_{j+1}, t) - \int_{C_j}^{C_{j+1}} \left| \frac{\partial f}{\partial C}(C, t) \right| dC \right) \quad (7)$$

and analogously for the clarification zone and the outlet zones. In Method G, we choose instead

$$F_j^{\text{num,G}} = F^{\text{num,G}}(C_j, C_{j+1}, t) := \begin{cases} -Q_{\text{e}}(t)C_{j+1}/A & \text{for } j = -2, -1, \\ -Q_{\text{e}}(t)C_{j+1}/A + G_j & \text{for } j = 0, \dots, j_{\text{f}} - 1, \\ Q_{\text{u}}(t)C_j/A + G_j & \text{for } j = j_{\text{f}}, \dots, N, \\ Q_{\text{u}}(t)C_j/A & \text{for } j = N + 1, N + 2, \end{cases} \quad (8)$$

where the Godunov formula applied to f_{bk} is

$$G_j = G_j(C_j, C_{j+1}) := \begin{cases} \min_{C_j \leq C \leq C_{j+1}} f_{\text{bk}}(C) & \text{if } C_j \leq C_{j+1}, \\ \max_{C_{j+1} \leq C \leq C_j} f_{\text{bk}}(C) & \text{if } C_j > C_{j+1}. \end{cases} \quad (9)$$

This formula is particularly easy to evaluate in the most relevant case that f_{bk} has precisely one local maximum (see Bürger et al., 2012).

2.4. The CFL condition and fully discrete scheme. Suppose that we want to simulate an SST over a time interval $[0, T]$ for a chosen layer thickness Δz . For the discretization in time of the system of ODEs (5), the time step Δt must be chosen such that the condition

$$\Delta t \leq \frac{1}{\frac{k_1}{\Delta z} + \frac{k_2}{\Delta z^2}} \quad (10)$$

is satisfied, where we define the constants

$$\begin{aligned} k_1 &:= \max_{0 \leq t \leq T} \frac{Q_f(t)}{A} + \max_{0 \leq C \leq C_{\max}} |f'_{\text{bk}}(C)|, \\ k_2 &:= 2 \left(\max_{0 \leq C \leq C_{\max}} d_{\text{comp}}(C) + \max_{-H \leq z \leq B, 0 \leq t \leq T} d_{\text{disp}}(z, Q_f(t)) \right). \end{aligned} \quad (11)$$

Here C_{\max} is a maximum concentration, chosen such that $f_{\text{bk}}(C) \approx 0 \approx f'_{\text{bk}}(0)$ for $C > C_{\max}$. Observe that for given Δz , inequality (10) yields an upper limit of the time step Δt that must be submitted into any ODE solver. A condition like (10) is known as a *CFL condition* (after Courant, Friedrichs & Lewy, 1928). This is a necessary condition to ensure stability of the numerical scheme.

The two numerical fluxes described above are only first-order accurate in space. Hence, for the time discretization, first-order accurate explicit Euler steps are usually sufficient. Let $t_n := n\Delta t$ and C_j^n be the approximate value of $C_j(t)$ at $t = t_n$. Then the fully discrete scheme can be written as the explicit marching formula

$$\begin{aligned} C_j^{n+1} &= C_j^n - \frac{\Delta t}{\Delta z} (F_j^{\text{num},n} - F_{j-1}^{\text{num},n}) + \frac{\Delta t}{\Delta z} (J_{\text{disp},j}^{\text{num},n} - J_{\text{disp},j-1}^{\text{num},n} + J_{\text{comp},j}^{\text{num},n} - J_{\text{comp},j-1}^{\text{num},n}) \\ &\quad + \frac{\Delta t}{\Delta z} \frac{Q_f(t_n) C_f(t_n)}{A} \delta_{j,j_f}, \quad j = -1, \dots, N+2. \end{aligned} \quad (12)$$

Here $F_j^{\text{num},n}$ is the value of F_j^{num} produced by replacing C_j and C_{j+1} by C_j^n and C_{j+1}^n , respectively. The dispersion and compression terms are given by the respective expressions

$$J_{\text{disp},j}^{\text{num},n} := d_{\text{disp}}(z_j, Q_f(t_n)) \frac{C_{j+1}^n - C_j^n}{\Delta z}, \quad (13)$$

$$J_{\text{comp},j}^{\text{num},n} := \gamma(z_j) \frac{D_{j+1}^{\text{num},n} - D_j^{\text{num},n}}{\Delta z}, \quad (14)$$

where $D_j^{\text{num},n}$ is either the exact or an approximate integrated compression coefficient

$$D(C) = \int_{C_c}^C d_{\text{comp}}(s) ds. \quad (15)$$

We refer to Bürger et al. (2012) for details on how to compute this. See also Section 4.6.

2.5. Constitutive relations and parameters for simulations. For the simulations we use the parameters $H = 1$ m, $B = 3$ m and $A = 400$ m². The maximum concentration for the CFL condition (10)–(11) is $C_{\max} = 20$ kg/m³. The constitutive functions f_{bk} and d_{comp} are chosen according to De Clercq et al. (2008) but with some changes of the parameter values:

$$f_{\text{bk}}(C) = \begin{cases} v_0 C e^{-rC} & \text{for } C < C_{\max}, \\ 0 & \text{for } C \geq C_{\max}, \end{cases} \quad (16)$$

$$d_{\text{comp}}(C) = \begin{cases} 0 & \text{for } C < C_c, \\ \frac{\rho_s \alpha f_{\text{bk}}(C)}{\Delta \rho g C (C - C_c + \beta)} & \text{for } C \geq C_c, \end{cases} \quad (17)$$

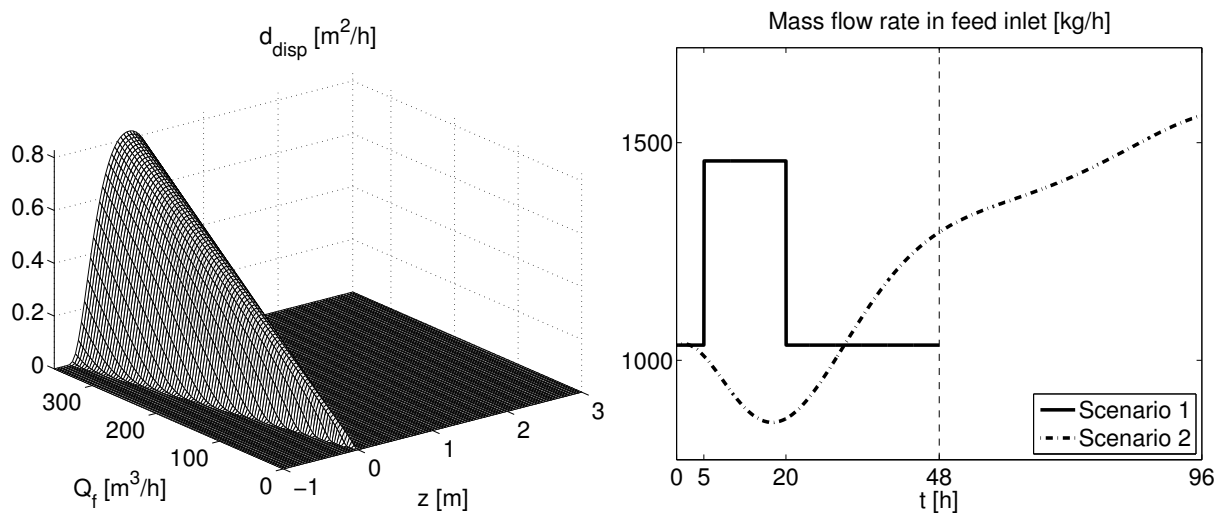


FIGURE 1. Graphs of functions used in the simulations of Scenarios 1 and 2. Left: The dispersion coefficient $d_{\text{disp}}(z, Q_f)$. Right: The solids loading $Q_f(t)C_f(t)$ in the feed inlet.

where $v_0 = 3.47 \text{ m/h}$, $r = 0.37 \text{ m}^3/\text{kg}$, $\alpha = 4.00 \text{ Pa}$ and $\beta = 4.00 \text{ kg/m}^3$. The density of the solids is $\rho_s = 1050 \text{ kg/m}^3$, the density difference between the solids and water is $\Delta\rho = 52 \text{ kg/m}^3$, the acceleration of gravity is $g = 9.81 \text{ m/s}^2$ and the critical concentration is $C_c = 6.00 \text{ kg/m}^3$. The third constitutive function d_{disp} is set to be increasing with the feed flow rate Q_f and assumed to be nonzero around the inlet only:

$$d_{\text{disp}}(z, Q_f) = \begin{cases} \alpha_1 Q_f \exp\left(\frac{-z^2/(\alpha_2 Q_f)^2}{1 - |z|/(\alpha_2 Q_f)}\right) & \text{for } |z| < \alpha_2 Q_f, \\ 0 & \text{for } |z| \geq \alpha_2 Q_f, \end{cases}$$

where $\alpha_1 = 0.0023 \text{ m}^{-1}$ and $\alpha_2 = 0.0025 \text{ h/m}^2$, see Figure 1 (left).

3. COMPARISON BETWEEN METHOD G AND METHOD EO

To compare Method G with Method EO, we use the same division of the z -axis for both. Therefore, we let the number of internal layers (within the SST) be $N = 10 \cdot 3^p$ for $p = 0, 1, \dots, 5$. The methods are compared by simulations of two scenarios starting at the same steady state (computed with Method EO). To illustrate the convergence and define suitable error measures, a reference solution was generated with Method EO using $N = 2430$ ($p = 5$) for each scenario. Subsequently, approximate solutions for $N = 10, 30, 90, 270$ and 810 were produced with both methods. The scenarios are constructed to demonstrate and compare the two methods and to show their robustness. Therefore, extreme variations in the concentrations and flow rates have been imposed.

Scenario 1. We start in a steady state with the feed flow rate $Q_f = 230 \text{ m}^3/\text{h}$, the feed concentration $C_f = 4.5 \text{ kg/m}^3$, the underflow rate $Q_u = 100 \text{ m}^3/\text{h}$ and with a sludge blanket in the thickening zone. At $t = 5 \text{ h}$, we impose a step increase in the solids loading in the

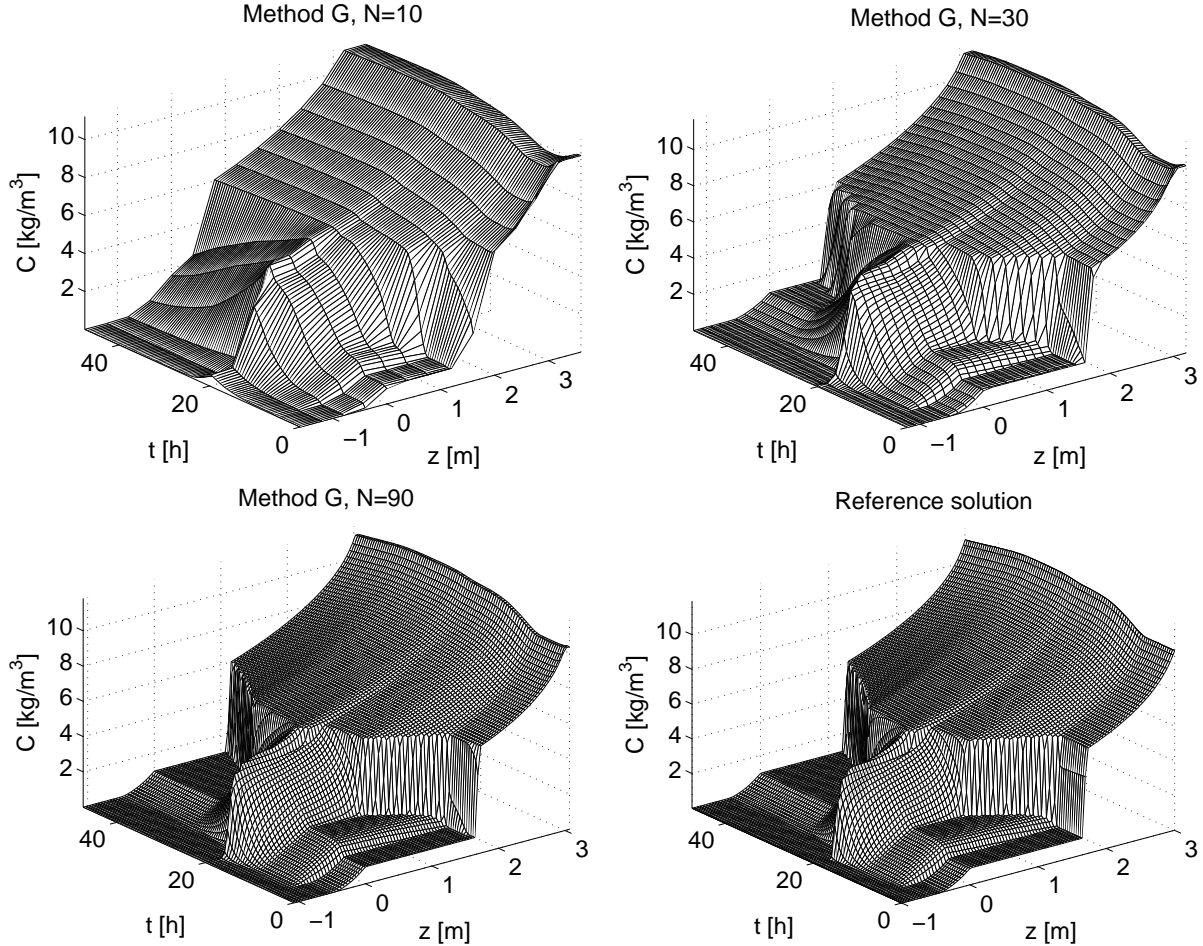


FIGURE 2. Four approximate solutions for Scenario 1. The reference solution in the lower right plot is computed with Method EO for $N = 2430$ internal layers, while the others are computed with Method G for 10, 30 and 90 internal layers.

feed inlet constructed by changing Q_f to $360 \text{ m}^3/\text{h}$, decreasing C_f by 10% and keeping the underflow rate constant, see Figure 1 (right). At $t = 20 \text{ h}$ all variables are returned to their initial values. The total simulation time is $T = 48 \text{ h}$.

Scenario 2. The same initial state as in Scenario 1 is used. Throughout the simulation, the underflow and effluent flow rates are kept proportional to the feed flow rate: $Q_u = \alpha_3 Q_f$ and $Q_e = (1 - \alpha_3) Q_f$, where $\alpha_3 = 10/23$ (i.e., the same ratio as in the initial state). The solids loading in the feed inlet is changed according to Figure 1 (right) with the feed flow rate Q_f oscillating around its initial value with period 24 h and amplitude $50 \text{ m}^3/\text{h}$. The total simulation time is $T = 96 \text{ h}$.

Results. A selection of numerical solutions generated by Method G for Scenario 1 is presented in Figure 2. The corresponding reference solution is shown in the lower right figure.

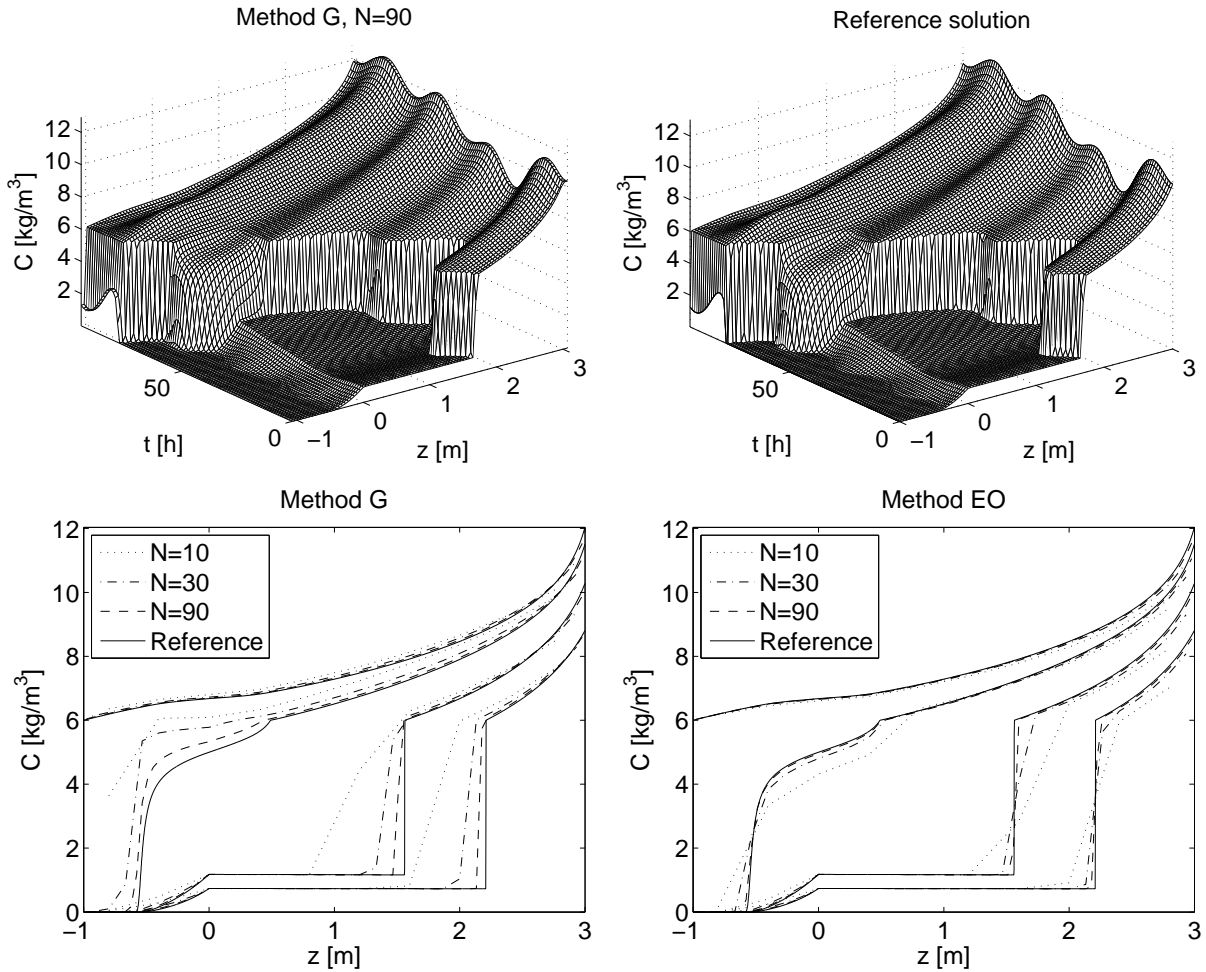


FIGURE 3. Scenario 2. Top: A simulation produced with Method G for $N = 90$ internal layers (left) and the reference solution (right). Bottom: Concentration profiles at $t = 20$ h, 40 h, 65 h and 96 h from the simulations produced with Method G (left) and Method EO (right) for $N = 10, 30$ and 90 internal layers.

It is evident how the approximate solution for $N = 10$ layers deviates from the reference solution, but as the number of layers increases the approximations clearly converge. The simulations for Scenario 2 are presented in a slightly different way in Figure 3.

In light of the convergence analysis for Method EO in Bürger et al. (2005), it is reasonable to assume that the reference solutions for $N = 2430$ internal layers are the ones closest to the true solution for the given input data in each scenario. In order to quantify the performance

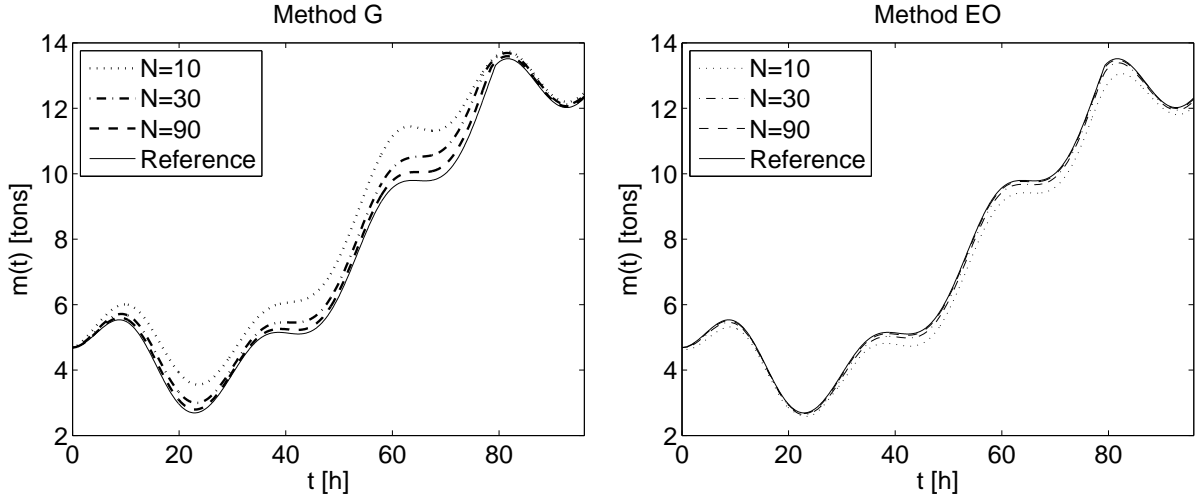


FIGURE 4. Masses for Scenario 2. The mass $m^N(t)$ for different number of internal layers are plotted together with $m^{\text{ref}}(t)$. Left: The underlying simulations are produced with Method G. Right: The underlying simulations are produced with Method EO.

of Method G compared with Method EO, the following error measures are used in Table 1:

$$e_C = \frac{\int_0^T \int_{-B}^H |C^N(z, t) - C^{\text{ref}}(z, t)| dz dt}{\int_0^T \int_{-B}^H C^{\text{ref}}(z, t) dz dt}$$

and

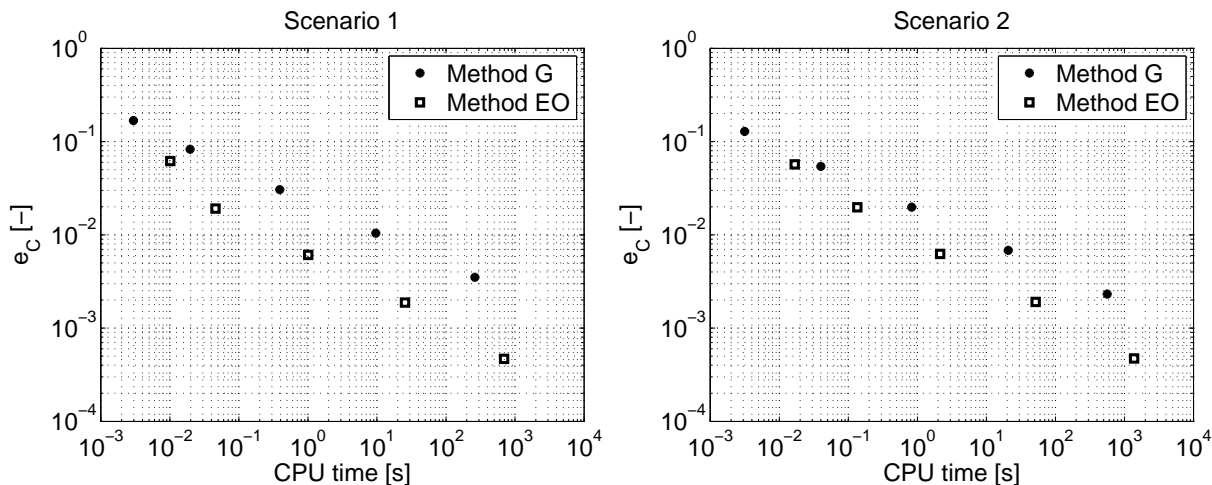
$$e_m = \frac{\int_0^T |m^N(t) - m^{\text{ref}}(t)| dt}{\int_0^T m^{\text{ref}}(t) dt}.$$

In the relative error e_C , C^N is a piecewise constant representation of the approximate solution generated over N internal layers by any of the two methods and C^{ref} is the reference solution restricted to the same grid by taking averages. In the relative mass error e_m , $m^N(t)$ and $m^{\text{ref}}(t)$ are the masses in the SST at time t derived from C^N and C^{ref} , respectively. Figure 4 shows the time variations for the masses in Scenario 2.

From the columns containing the CPU times in Table 1, it is seen that Method G is faster than Method EO for any fixed N . However, this comes at the price of less accurate numerical approximations, which is clear from both error measures. In fact, the e_C versus CPU time diagrams of Figure 5 illustrate that for both scenarios, the data points corresponding to Method EO can be interpolated to give a rough line that lies below that for the results obtained with Method G. This means that Method EO requires less CPU time to produce

TABLE 1. Errors and CPU times for simulations with different number of layers N .

	Scenario 1				Scenario 2		
	N	e_C [-]	e_m [-]	CPU time [s]	e_C [-]	e_m [-]	CPU time [s]
Method G	10	1.68E-1	1.30E-1	2.96E-3	1.29E-1	1.09E-1	3.14E-3
	30	8.28E-2	7.24E-2	1.96E-2	5.42E-2	4.70E-2	3.99E-2
	90	3.06E-2	2.72E-2	3.90E-1	1.98E-2	1.73E-2	8.28E-1
	270	1.04E-2	9.37E-3	9.63E+0	6.82E-3	6.04E-3	2.07E+1
	810	3.51E-3	3.26E-3	2.62E+2	2.32E-3	2.14E-3	5.63E+2
Method EO	10	6.19E-2	3.90E-2	1.01E-2	5.71E-2	4.20E-2	1.67E-2
	30	1.91E-2	1.08E-2	4.57E-2	1.97E-2	1.38E-2	1.35E-1
	90	6.10E-3	3.82E-3	1.01E+0	6.25E-3	4.28E-3	2.14E+0
	270	1.88E-3	1.08E-3	2.55E+1	1.91E-3	1.35E-3	5.17E+1
	810	4.68E-4	2.77E-4	6.95E+2	4.73E-4	3.31E-4	1.38E+3

FIGURE 5. The error e_C versus CPU time for different values of N according to Table 1.

a numerical solution with an error below a certain threshold, which means that Method EO is more efficient for both scenarios.

4. PITFALLS AND UNSUITABLE METHODS

4.1. Monotone numerical fluxes. Method EO gives rise to approximate solutions that converge to the physically relevant solution of the governing PDE (1) as $\Delta t \rightarrow 0$ and $\Delta z \rightarrow 0$, provided that Δt and Δz satisfy the CFL condition (10), (11). Although it has not yet been proved, the comparisons by simulation in Section 3, together with the fact that the fluxes $F^{\text{num,EO}}$ and $F^{\text{num,G}}$ are equal in many cases (although the formulas are quite different), indicate strongly that Method G is also reliable. The decisive property that permits to prove such a convergence result (see Bürger et al. 2005, 2010) is the monotonicity of the numerical flux F^{num} , i.e., the function F^{num} is non-decreasing in its first argument and

non-increasing in its second. For the fluxes $F^{\text{num,EO}}$ and $F^{\text{num,G}}$ defined by (7) and (8), respectively, it turns out that for fixed n , and under the CFL condition (10), (11), the right-hand side of the discrete scheme as a whole, (12), is a non-decreasing function of the three values C_{j-1}^n , C_j^n and C_{j+1}^n . The convergence of monotone schemes to the physically relevant solution, the entropy solution, of a scalar conservation law was first demonstrated by Harten et al. (1976) and Crandall & Majda (1980), and has also been established for the special case of the present clarifier-thickener model arising from setting to zero d_{comp} and d_{disp} (Bürger et al. 2004, 2010). On the other hand, if these terms are present and we assume (for simplicity) that the coefficients of (1) are constant in time and (10) is satisfied, then (12) equipped with the Engquist-Osher flux is still a three-point monotone scheme that converges to the (properly defined) entropy solution, see Bürger et al. (2005).

4.2. The Lax-Friedrichs numerical flux is consistent and monotone but unsuitable. The importance of monotonicity and the fact that both Method EO and Method G give rise to monotone schemes raises the question whether other monotone, and possibly easier to evaluate, fluxes could be substituted for $F^{\text{num,EO}}$ or $F^{\text{num,G}}$. One such flux is the Lax-Friedrichs numerical flux, which, applied on the batch-settling flux f_{bk} reads:

$$F^{\text{num,LxF}}(C_j, C_{j+1}) := \frac{\Delta z}{2\Delta t}(C_j - C_{j+1}) + \frac{1}{2}(f_{\text{bk}}(C_j) + f_{\text{bk}}(C_{j+1})). \quad (18)$$

It can easily be checked that this flux is consistent, i.e., it satisfies (6), and is monotone under the CFL condition (10). In contrast to $F^{\text{num,EO}}$ and $F^{\text{num,G}}$, the numerical flux $F^{\text{num,LxF}}$ has the apparent advantage that it can be evaluated without the necessity to keep track of the extrema of f_{bk} , and it is tempting to consider $F^{\text{num,LxF}}$ as a serious alternative. However, the whole scheme (12) is not monotone with $F^{\text{num}} = F^{\text{num,LxF}}$ (unless $d_{\text{comp}} = d_{\text{disp}} \equiv 0$). In fact, differentiating (12), we have

$$\frac{\partial C_j^{n+1}}{\partial C_j^n} = -2\mu(d_{\text{comp}}(C_j^n) + d_{\text{disp}}(z_j, Q_f(t_n))),$$

which may be negative irrespective of any CFL condition. This indicates an unstable behaviour; simulations deteriorate. Thus, the Engquist-Osher or Godunov flux cannot be replaced by an arbitrary monotone flux.

4.3. The Stenstrom-Vitasovic-Takács flux is consistent but unsuitable (entropy violating). Jeppsson & Diehl (1996) demonstrated the advantages of the Godunov flux compared with the minimum-flux formula in the well-known method by Takács et al. (1991). The method was originally presented by Vitasovic (1989), who utilized the minimum-flux formula by Stenstrom (1976):

$$S_j = \min(f_{\text{bk}}(C_j), f_{\text{bk}}(C_{j+1})). \quad (19)$$

Hence, this flux could replace G_j in (8) to obtain a total numerical flux. This numerical flux is consistent, which is easily seen by setting $C_j = C_{j+1}$. However, it is not generally monotone. For example, if $f_{\text{bk}}(C_j) < f_{\text{bk}}(C_{j+1})$ and $f'_{\text{bk}}(C_j) < 0$, then $\partial S_j / \partial C_j^n = f'_{\text{bk}}(C_j) < 0$. Furthermore, it may produce a solution that does not satisfy the entropy condition. This was demonstrated by Bürger et al. (2011) by an example where an unphysical discontinuity (it does not satisfy the entropy condition) is stable when simulating with the flux S_j .

An explanation for the success of Takács' simulation model during normal operating conditions is the following. For an ordinary batch sedimentation test where the concentration is non-decreasing as a function of depth, $S_j = G_j$ holds, when f_{bk} is a unimodal function (has only one local maximum). Therefore, standard batch sedimentation tests can be simulated correctly with S_j . Our algorithm for the implementation of Method G (Bürger et al., 2012) has the feature that it can be seen as an extension of (19).

For continuous sedimentation, the concentration is also normally non-decreasing with depth, and the Takács method often works satisfactorily. However, during extreme events, such as storm weather, the concentration distribution may be decreasing with depth, then the Takács method fails, as our Simulation GvT shows.

Simulation GvT (Godunov versus Takács). In order to compare the numerical flux (19) in Takács' method with Godunov's flux, we turn off the other effects; $d_{\text{disp}} \equiv 0$ and $d_{\text{comp}} \equiv 0$. Assume that the flows to the SST have been turned off for some time and the sludge in the SST has settled. At $t = 0$, we assume that there is a concentration of 15 kg/m^3 at the bottom of the thickening zone and clear water above. We let the influent variables be constant in time and the volumetric underflow rate small: $Q_f = 405 \text{ m}^3/\text{h}$, $Q_u = 5 \text{ m}^3/\text{h}$, and hence $Q_e = 400 \text{ m}^3/\text{h}$, $C_f = 4.0 \text{ kg/m}^3$. The result of the simulations with different number of layers are shown in Figures 6 and 7. Correct approximations of the solution are produced by Method G. It is in fact possible to construct the unique entropy-satisfying solution; see Diehl (2005; Section 4.7.4). Because of the low volumetric underflow rate, solids will build up around the inlet in both clarification and thickening zones. Immediately, particles start to settle down to the sludge blanket, which they reach within half an hour. In the numerical solutions with Takács' method, the particles move much slower downwards above an unphysical discontinuity. They only follow the downward bulk flow and reach the sludge blanket after 2 hours. This clearly illustrates a physically incorrect situation. Note that the approximate solution satisfies the conservation of mass, but not the entropy condition. A second incorrectness of the Takács method is the build-up of particles just above the sludge blanket for the simulations with $N = 30$ and 90 . The third incorrectness is the ripple that appears above the sludge blanket in the thickening zone as the number of layers increases. A fourth incorrectness is the speed of the rising discontinuity in the clarification zone, which is too high for the Takács method. The correct concentration building up in the clarification zone, 3.80 kg/m^3 , is in fact slightly less than the feed concentration $C_f = 4.0 \text{ kg/m}^3$, see Diehl (2005; Section 4.7.4). All in all, the simulations produced by the Takács method are qualitatively different for different number of layers – a feature that makes it useless. In addition, it is different from the correct solution.

4.4. Parameters in the numerical method. In a consistent modelling methodology (Bürger et al., 2011), all physical phenomena should be captured first in the model equation (1) or equivalently (3), which contains the constitutive relations with its model parameters. Any numerical method for simulation should then be closely related to the model equation. In particular, the only model parameters allowed in the numerical method are inherited from the constitutive relations. The purpose of any numerical method is only to produce approximate solutions of the PDE. Introducing parameters directly into the numerical methods means that one imposes assumptions on the solution, which may be unphysical. Numerical

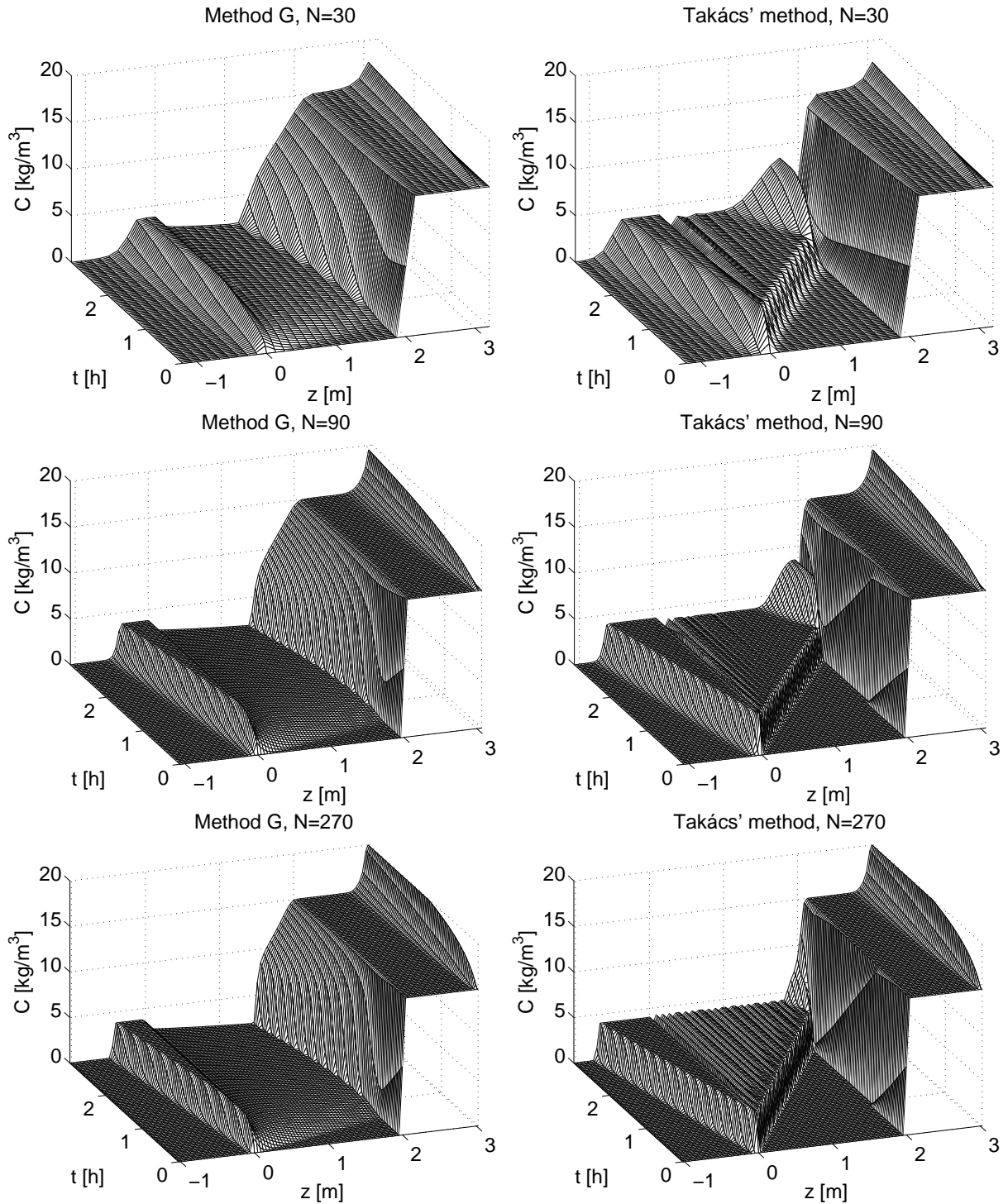


FIGURE 6. 3D graphs of Simulation GvT.

solutions should instead be the output results of the physical principles and the assumed

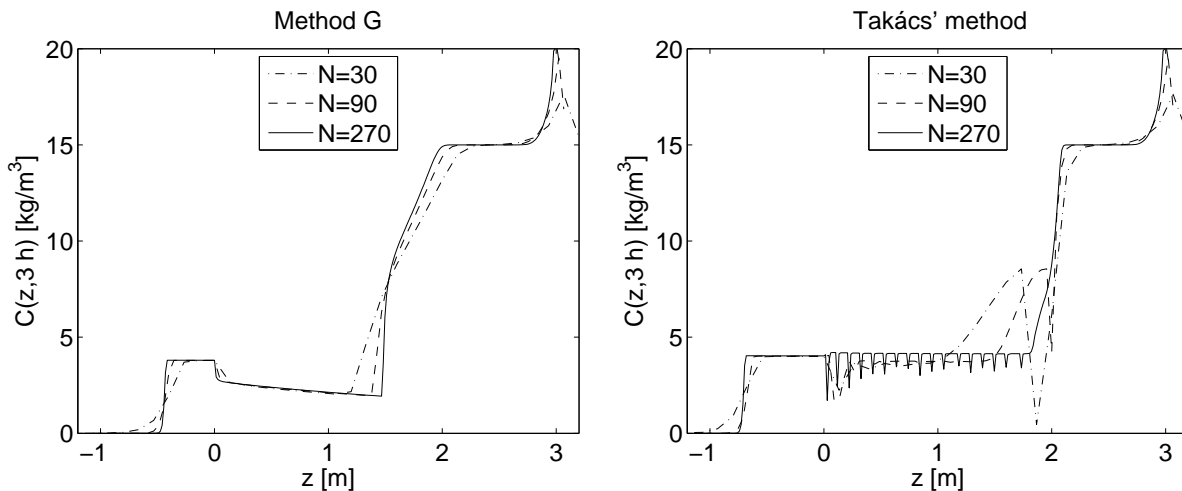


FIGURE 7. The concentration profile at $t = 3$ h of Simulation GvT.

constitutive relations. Examples of such parameters which cannot be found in the corresponding model equation are the threshold concentration in the clarification zone by Takács et al. (1991), the reduction factor multiplied with the downward bulk velocity Q_u/A by Plósz et al. (2007, 2011), and factors in the numerical flux to account for compression by Abusam & Keesman (2009).

4.5. Boundary conditions and heuristic assumptions. The advantage of the model formulation that the governing equation (1) or (3) should hold on the entire real line, i.e., the SST and the outlet pipes are divided into four zones, is that no boundary conditions need to be imposed. In fact, no extra boundary conditions must be imposed, since this means potentially unphysical assumptions on the solution. The conservation of mass (3) should hold in any interval $[z_1, z_2]$ of the real axis, also when such an interval contains one of the outlet locations. Hence, the correct boundary “condition” is that the flux of particles leaving the SST is equal to the flux of particles in the outlet pipe just outside the SST. The outlet concentrations C_e and C_u are part of the solution, i.e., they are model outputs which should be delivered automatically without any extra assumption. Note that the special case of batch settling in a column is included within this setting. Then $Q_e = Q_u = 0$, and since we have neither compression nor dispersion in the effluent and underflow zones, at the top and bottom respectively, the total flux Φ in (4) is zero outside the SST, and hence also at the top and bottom inside the SST.

In many of the published simulation methods for SSTs, extra boundary conditions are assumed. The most common assumption is that the concentrations in the outlet pipes are equal to the concentrations in the top and bottom layer, respectively (Abusam & Keesman, 2009; David et al., 2009a, b; Dupont & Dahl, 1995; Hamilton et al., 1992; Härtel & Pöpel, 1992; Koehne et al., 1995; Lee et al., 2006; Nocoń, 2006; Otterpohl & Freund, 1992; Ozinsky et al., 1994; Plósz et al., 2007, 2011; Stepova & Kalugin, 2011; Takács et al., 1991; Verdickt et al., 2005; Vitasovic, 1989; Watts et al., 1996; Wett, 2002). In other words, one assumes that the concentration is continuous across the SST boundaries and this is done without

any reference to the solution of the model PDE. Instead, the conservation of mass implies that the total flux Φ , see (4), is continuous over the boundaries. In fact, assuming that the concentration is continuous over the boundaries may violate the conservation of mass as can be seen with the following example. Consider the hyperbolic case when $d_{\text{comp}} = d_{\text{disp}} \equiv 0$ and assume that $C^{\text{top}} := C(-H + 0, t) > 0$ is the concentration at the top of the clarification zone at time t . Then the total flux at the top of the clarification zone inside the SST is

$$\Phi \left(C^{\text{top}}, \frac{\partial C}{\partial z}, -H + 0, t \right) = f_{\text{bk}}(C^{\text{top}}) - \frac{Q_e C^{\text{top}}}{A}$$

and in the effluent pipe

$$\Phi \left(C_e, \frac{\partial C}{\partial z}, -H - 0, t \right) = -\frac{Q_e C_e}{A},$$

since there is only bulk flow in the effluent pipe (it is impossible for any gravity settling to make particles move back into the SST as they have left it). The conservation of mass, i.e., the flux is continuous, yields

$$f_{\text{bk}}(C^{\text{top}}) - Q_e C^{\text{top}}/A = -Q_e C_e/A \quad \iff \quad C_e = C^{\text{top}} - \frac{A f_{\text{bk}}(C^{\text{top}})}{Q_e}. \quad (20)$$

Hence, the conservation of mass implies that the effluent concentration C_e is strictly less than the one inside the SST C^{top} . Erroneously setting $C_e := C^{\text{top}}$ thus means that extra mass is created from nowhere.

It should be mentioned that (20) holds in steady state and in the hyperbolic case when $d_{\text{comp}} = d_{\text{disp}} \equiv 0$. The difficulty is to establish C^{top} (and the corresponding bottom concentration) from the exact solution of the PDE during dynamic operation. Such formulas have been presented by Diehl (1996), which imply the numerical update formulas presented by Diehl & Jeppsson (1998). In our simulation model, however, when the second-order derivative terms are sometimes present and sometimes not, we prefer the straightforward numerical implementation by using the four extra layers outside the SST.

As has also been noticed by Bürger et al. (2005), all simulations indicate that in regions where the second-order terms are nonzero in the governing equation (1), the solution is smooth also over boundaries. For the simulation of SSTs where the concentration at the bottom in most cases is greater than the critical one C_c , the underflow concentration C_u equals the bottom concentration inside the SST. However, at the top it is likely that there is no compression present. An example where there is a discontinuity at the effluent location between the effluent concentration C_e and $C^{\text{top}} = C_c$ is provided in Figure 3 for $t \gtrsim 80$ h.

There are attempts to let the feed inlet location depend on the solution itself in the numerical algorithm (Watts et al., 1996; Plósz et al., 2007, 2011). The solution is always dependent on the feed location, wherefore it is doubtful that such an approach can be formulated as any well-posed mathematical problem (model PDE plus initial data).

We are forced to mention that the number of layers N should only be a parameter that controls the quality of approximation of the exact solution of the model PDE. The number of layers is not a parameter to be adjusted to a particular physical reality (cf. Stricker et al., 2007).

In the paper by Stricker et al. (2007), the effect of compression is modelled by introduction of extra terms in the batch settling flux function f_{bk} . Although this is in agreement with a consistent modelling methodology (parameters should be introduced in the constitutive assumptions only), this is unsuitable from the commonly known physical insight that such a constitutive assumption necessarily involves also the gradient of the concentration.

4.6. Discretization of the dispersion and compression fluxes. Finally, let us comment on the on proper discretization of the second-order derivative terms on the right-hand side of (1), or rather, the dispersion and compression fluxes in (4). Since the dispersion coefficient $d_{\text{disp}}(z, Q_f)$ is a continuous function and does not depend on the solution C , the corresponding term only means a smoothing of the solution. A straightforward difference approximation; see (13), is therefore unharmed.

The modelling of the compression of particles above a certain critical concentration, or gel point, $C_c > 0$, may well imply that the compression coefficient $d_{\text{comp}}(C)$ has a discontinuity at $C = C_c$. The case that should be discussed carefully occurs thus when $d_{\text{disp}} \equiv 0$ and $d_{\text{comp}}(C)$ vanishes on a C -interval of positive length but is positive elsewhere. We may focus on the typical compression coefficient (17). Then the governing equation (1) is strongly degenerate parabolic since it degenerates to a first-order hyperbolic type wherever the solution assumes values $C < C_c$. This behaviour demands some care in the discretization. Roughly speaking, convergence analyses for numerical schemes for strongly degenerate parabolic equations (Evje & Karlsen, 2000; see also Bürger & Karlsen, 2001) suggest that the discretization (12), (14), which boils down to

$$\left(d_{\text{comp}}(C) \frac{\partial C}{\partial z} \right) (z_j, t_n) = \frac{\partial D(C)}{\partial z} (z_j, t_n) = \frac{D(C_{j+1}^n) - D(C_j^n)}{\Delta z} + \mathcal{O}(\Delta z), \quad (21)$$

ensures that the corresponding scheme converges to the appropriate physically relevant (entropy) solution of (1) as $\Delta t, \Delta z \rightarrow 0$, provided the CFL condition (10) is satisfied. The formula (21) is called *conservative discretization*. Note that the discretization (21) ensures that the final scheme is monotone under the CFL condition.

The salient point we are making here is that there are other “natural” discretizations, for example (cf. Watts et al., 1996)

$$\left(d_{\text{comp}}(C) \frac{\partial C}{\partial z} \right) (z_j, t_n) \approx d_{\text{comp}} \left(\frac{C_j^m + C_{j+1}^m}{2} \right) \frac{C_{j+1}^m - C_j^m}{\Delta z}. \quad (22)$$

While this “non-conservative” discretization (or others such as the one proposed by Stepova & Kalugin (2011; Eq. (47))) can well be employed for strictly parabolic equations with $d_{\text{comp}} > 0$, which have smooth solutions, in the strongly degenerate case (22) will in general produce wrong discontinuous solutions. We demonstrate this by the following example.

Simulation D. The simulation demonstrates the fill-up of an SST, which is initially filled with only water. We turn off the dispersion effect ($\alpha_1 = 0$) and let the other parameters in the constitutive relations be as in Section 2.5. We use the following time-independent values: $Q_f = 250 \text{ m}^3/\text{h}$, $Q_u = 80 \text{ m}^3/\text{h}$, $Q_e = 170 \text{ m}^3/\text{h}$ and $C_f = 4 \text{ kg}/\text{m}^3$. Correct approximate solutions are presented to the left in Figure 8. It contains a typical sludge blanket with the critical concentration $C_c = 6 \text{ kg}/\text{m}^3$ just below it. In fact, the PDE theory yields that the

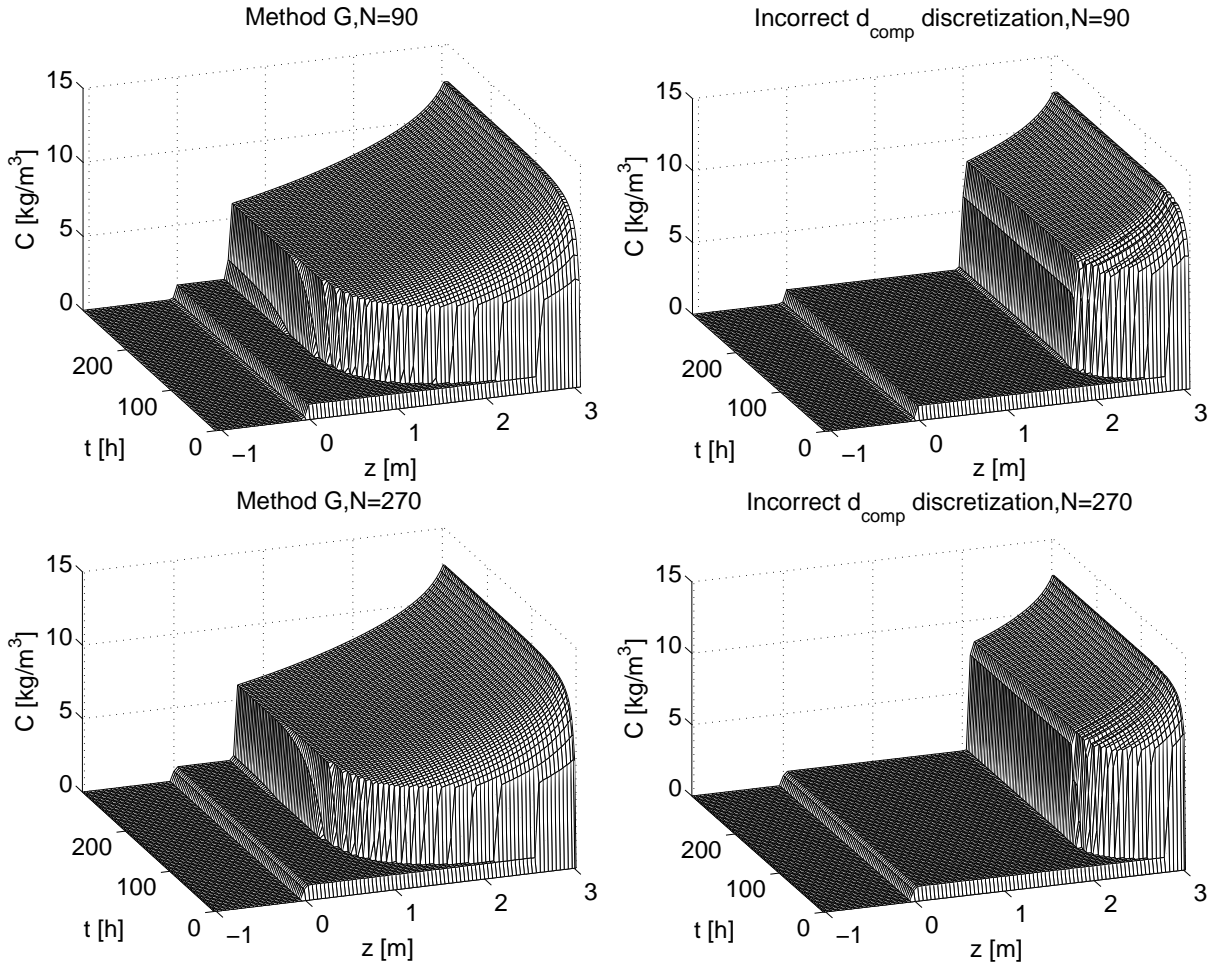


FIGURE 8. 3D graphs of Simulation D.

only entropy-satisfying discontinuities that may arise in the solution must have lower and higher concentration values in the interval $[0, C_c]$. To the right in Figure 8, simulations are shown with the incorrect discretization (22) and we can infer three incorrectnesses. The location of the sludge blanket is wrong, the concentration below the discontinuity is greater than C_c and in the transient part of the solution, a non-monotone behaviour of the numerical method can be seen. It should be mentioned that all simulations have been done with the CFL condition (10). The problem with the incorrect discretization is that there is no CFL condition with $\Delta t / (\Delta z)^2$ bounded because of the appearance of a term containing $d'_{\text{comp}}(C)$, which is unbounded near $C = C_c$. Simulations with much smaller time steps show, however, the same behaviour as in Figure 8.

5. CONCLUSIONS

We recommend the use of reliable numerical methods for simulation. This paper illustrates how recent results of numerical analysis can be used for the practical application to the simulation of SSTs. Applied mathematical research has led to several alternative methods,

represented here by Method G and Method EO, which are both sound in the sense that they converge to the solution of the PDE as the discretization tends to zero. For Method EO this has been proved by Bürger et al. (2005) and the comparisons here indicate strongly that this holds for Method G as well. The choice of method to be implemented in a simulator is subject to several competing principles. As our results show, for a given value of N , Method G produces a numerical solution faster than Method EO, but the value of this advantage is questionable since Method EO is more efficient than Method G in reducing the numerical error. In other words, the disadvantage of larger CPU times associated with Method EO is more than compensated by the gain in quality of numerical solutions if compared with Method G. This quality difference is a result of the application of the numerical flux formula to the total flux and the batch settling flux, respectively, rather than the choice of numerical flux formula (Engquist-Osher or Godunov). An aspect that speaks in favour of Method G is its ease of implementation.

We have argued and demonstrated some pitfalls and unsuitable approaches when deriving simulation models for SSTs. An erroneous but common approach is to try to formulate an SST model in terms of a numerical method directly. In many cases found in the literature, this has led to unreliable simulation methods. The main reason for this is the nonlinear behaviour of the continuous sedimentation process, which when consistently modelled, needs PDE theory and advanced numerical analysis for the derivation of a reliable simulation model.

ACKNOWLEDGMENTS

RB acknowledges partial support by Fondecyt project 1090456, and BASAL project CMM, Universidad de Chile and Centro de Investigación en Ingeniería Matemática (CI²MA), Universidad de Concepción. SD acknowledges the Foundation for Engineering Scientific Research to the Memory of J. Gust. Richert, SWECO AB, Sweden. SF acknowledges the Crafoord Foundation, Sweden (grant 20110535). IN thanks the Flemish Fund for Scientific Research (Project G.A051.10).

NOMENCLATURE

A	cross-sectional area of SST [m^2]
B	depth of thickening zone [m]
C	concentration in SST [kg/m^3]
C_c	critical concentration [kg/m^3]
C_j	average of C over layer j [kg/m^3]
C_{\max}	maximum concentration [kg/m^3]
D	primitive of d_{comp} [$\text{kg}/(\text{m}^2\text{s})$]
F	(convective) flux function [$\text{kg}/(\text{m}^2\text{s})$]
G	Godunov numerical flux [$\text{kg}/(\text{m}^2\text{s})$]
H	height of clarification zone [m]
J_{comp}	compressive flux [$\text{kg}/(\text{m}^2\text{s})$]
J_{disp}	dispersive flux [$\text{kg}/(\text{m}^2\text{s})$]
N	number of layers of SST [$-$]

Q	volumetric flow rate [m^3/s]
d_{comp}	compression function [m^2/s]
d_{disp}	dispersion function [m^2/s]
f_{bk}	Kynch batch flux density function [$\text{kg}/(\text{m}^2\text{s})$]
g	acceleration of gravity [m/s^2]
j	layer index [–]
r	parameter in equation for f_{bk} [m^3/kg]
t	time [s]
v_0	settling velocity of a single particle in unbounded fluid [m/s]
v_{hs}	hindered settling velocity
z	depth from feed level in SST [m]

Greek letters.

ΔC	stepsize of discretization of C -axis [kg/m^3]
Δt	time step of numerical method [s]
Δz	layer width of numerical method [m]
$\Delta \rho$	solid-fluid density difference [kg/m^3]
Φ	(total) flux [$\text{kg}/(\text{m}^2\text{s})$]
α	parameter in compression function [Pa]
α_1	parameter in dispersion coefficient [m^{-1}]
α_2	parameter in dispersion coefficient [s/m^2]
β	parameter in compression function [kg/m^3]
γ	characteristic function, equals 1 inside and 0 outside SST
δ	Dirac delta distribution [m^{-1}]
ρ_s	density of solids [kg/m^3]

Subscripts.

e	effluent
f	feed
u	underflow

Superscripts.

num	numerical (convective or diffusive) flux
-----	--

REFERENCES

- Abusam, A., & Keesman, K.J. (2009). Dynamic modeling of sludge compaction and consolidation processes in wastewater secondary settling tanks. *Water Environment Research*, 81, 51–56.
- Bürger, R., & Karlsen, K.H. (2001). On some upwind schemes for the phenomenological sedimentation-consolidation model. *Journal of Engineering Mathematics*, 41, 145–166.

- Bürger, R., Karlsen, K.H., Risebro, N.H., & Towers, J.D. (2004). Well-posedness in BV_t and convergence of a difference scheme for continuous sedimentation in ideal clarifier-thickener units. *Numerische Mathematik*, *97*, 25–65.
- Bürger, R., Karlsen, K.H., Torres, H., & Towers, J.D. (2010). Second-order schemes for conservation laws with discontinuous flux modelling clarifier-thickener units. *Numerische Mathematik*, *116*, 579–617.
- Bürger, R., Karlsen, K.H., & Towers, J.D. (2005). A model of continuous sedimentation of flocculated suspensions in clarifier-thickener units. *SIAM Journal on Applied Mathematics*, *65*, 882–940.
- Bürger, R., Diehl, S., & Nopens, I. (2011). A consistent modelling methodology for secondary settling tanks in wastewater treatment. *Water Research*, *45*, 2247–2260.
- Bürger, R., Diehl, S., Farås, S., Nopens, I., & Torfs, E. (2012). A consistent modelling methodology for secondary settling tanks: A reliable numerical method. Preprint, CP²MA, Universidad de Concepción.
Available under <http://www.ci2ma.udec.cl/publicaciones/prepublicaciones/>.
- Courant, R., Friedrichs, K., & Lewy, H. (1928). Über die partiellen Differenzgleichungen der mathematischen Physik. *Mathematische Annalen*, *100*, 32–74.
- Crandall, M.G., & Majda, A. (1980). Monotone difference approximations for scalar conservation laws. *Mathematics of Computation*, *34*, 1–21.
- David, R., Saucez, P., Vassel, J.-L., & Vande Wouwer, A. (2009a). Modeling and numerical simulation of secondary settlers: A method of lines strategy. *Water Research*, *43*, 319–330.
- David, R., Vassel, J.-L., & Vande Wouwer, A. (2009b). Settler dynamic modeling and MATLAB simulation of the activated sludge process. *Chemical Engineering Journal*, *146*, 174–183.
- Diehl, S. (1996). A conservation law with point source and discontinuous flux function modelling continuous sedimentation. *SIAM Journal on Applied Mathematics*, *56*, 388–419.
- Diehl, S. (2005). Operating charts for continuous sedimentation II: Step responses. *Journal of Engineering Mathematics*, *53*, 139–185.
- Diehl, S. (2009). A uniqueness condition for nonlinear convection-diffusion equations with discontinuous coefficients. *Journal of Hyperbolic Differential Equations*, *6*, 127–159.
- Diehl, S., & Jeppsson, U. (1998). A model of the settler coupled to the biological reactor. *Water Research*, *32*, 331–342.
- De Clercq, J., Nopens, I., Defrancq, J., & Vanrolleghem, P.A. (2008). Extending and calibrating a mechanistic hindered and compression settling model for activated sludge using in-depth batch experiments. *Water Research*, *42*, 781–791.
- Dupont, R., & Dahl, C. (1995). A one-dimensional model for a secondary settling tank including density current and short-circuiting. *Water Science and Technology*, *31*, 215–224.
- Engquist, B., & Osher, S. (1981). One-sided difference approximations for nonlinear conservation laws. *Mathematics of Computation*, *36*, 321–351.

- Evje, S., & Karlsen, K.H. (2000). Monotone difference approximations of BV solutions to degenerate convection-diffusion equations. *SIAM Journal on Numerical Analysis*, *37*, 1838–1860.
- Godunov, S.K. (1959). A difference method for numerical calculation of discontinuous solutions of the equations of hydrodynamics. *Matematicheskii Sbornik. Novaya Seriya*, *47*, 271–306 (in Russian).
- Guo, Y., Hu, Y., & Li, B. (2010). Application analysis of one-dimensional sedimentation model. IEEE Xplore paper, Fourth International Conference on Bioinformatics and Biomedical Engineering, Chengdu, China, June, 18–20.
- Härtel, L., & Pöpel, H.J. (1992). A dynamic secondary clarifier model including processes of sludge thickening. *Water Science and Technology*, *25*, 267–284.
- Hamilton, J., Jain, B., Antoniou, P., Svoronos, S.A., Koopman, B., & Lyberatos, G. (1992). Modeling and pilot-scale experimental verification for predenitrification process. *Journal of Environmental Engineering*, *118*, 38–55.
- Harten, A., Hyman, J.M., & Lax, P.D. (1976). On finite-difference approximations and entropy conditions for shocks. *Communications in Pure and Applied Mathematics*, *29*, 297–322.
- Holden, H., & Risebro, N.H. (2007). *Front Tracking for Hyperbolic Conservation Laws*. Corrected 2nd printing. Springer-Verlag, New York.
- Jeppsson, U., & Diehl, S. (1996). An evaluation of a dynamic model of the secondary clarifier. *Water Science and Technology*, *34(5–6)*, 19–26.
- Koehne, M., Hoen, K., & Schuhen, M. (1995). Modelling and simulation of final clarifiers in wastewater treatment plants. *Mathematics and Computers in Simulation*, *39*, 609–616.
- Lee, T.T., Wang, F.Y., & Newell, R.B. (2006). Advances in distributed parameter approach to the dynamics and control of activated sludge processes for wastewater treatment. *Water Research*, *40 (5)*, 853–869.
- LeVeque, R.J. (1992). *Numerical Methods for Conservation Laws*, Second Ed., Birkhäuser Verlag, Basel.
- LeVeque, R.J. (2002). *Finite Volume Methods for Hyperbolic Problems*. Cambridge University Press, Cambridge, UK.
- Nocoń, W. (2006). Mathematical modelling of distributed feed for continuous sedimentation. *Simulation Modelling Practice and Theory*, *14*, 493–505.
- Otterpohl, R., & Freund, M. (1992). Dynamic models for clarifiers of activated sludge plants with dry and wet weather flows. *Water Science and Technology*, *26(5–6)*, 1391–1400.
- Ozinsky, A.E., Ekama, G.A., & Reddy, B.D. (1994). Mathematical simulation of dynamic behaviour of secondary settling tanks. Technical Report W85. Dept. of Civil Engineering, University of Cape Town, South Africa.
- Plósz, B.G., Weiss, M., Printemps, C., Essemiani, K., & Meinhold, J. (2007). One-dimensional modelling of the secondary clarifier—factors affecting simulation in the clarification zone and the assessment of the thickening flow dependence. *Water Research*, *41*, 3359–3371.
- Plósz, B.G., Nopens, I., De Clercq, J., Benedetti, L., & Vanrolleghem, P.A. (2011). Shall we upgrade one-dimensional secondary settler models in WWTP simulators? An

- assessment of model structure uncertainty and its propagation. *Water Science and Technology*, *63*(8), 1726–1738.
- Stenstrom, M.K. (1976). A dynamic model and computer compatible control strategies for wastewater treatment plants. PhD dissertation, Clemson University, Clemson, South Carolina, USA.
- Stepova, N. & Kalugin, Y. (2011). Mathematical modelling of a secondary clarifier with a cone-shaped bottom. *International Journal of Fluid Mechanics Research*, *38*, 458–478.
- Stricker, A.-E., Takács, I., & Marquot, A. (2007). Hindered and compression settling: parameter measurement and modelling. *Water Science and Technology*, *56*(12), 101–110.
- Takács, I., Patry, G.G., & Nolasco, D. (1991). A dynamic model of the clarification-thickening process. *Water Research*, *25*, 1263–1271.
- Verdickt, L.B., Smets, I.Y., & Van Impe, J.F. (2005). Sensitivity analysis of a one-dimensional convection-diffusion model for secondary settling tanks. *Chemical Engineering Communications*, *192*, 1567–1585.
- Vitasovic, Z.Z. (1989). Continuous settler operation: A dynamic model. In Patry, G.G., & Chapman, D. (editors), *Dynamic Modelling and Expert Systems in Wastewater Engineering*, pp. 59-81. Lewis, Chelsea, MI, USA.
- Watts, R.W., Svoronos, S.A., & Koopman, B. (1996). One-dimensional modeling of secondary clarifiers using a concentration and feed velocity-dependent dispersion coefficient. *Water Research*, *30*, 2112–2124.
- Wett, B. (2002). A straight interpretation of the solids flux theory for a three-layer sedimentation model. *Water Research*, *36*, 2949–2958.